Astron. Astrophys. 317, 925–928 (1997)

ASTRONOMY
AND
ASTROPHYSICS

Relation between DIFOS "irradiance" data and solar activity

K. Pflug[1], **V.N. Obridko**[2], **K. Arlt**[1], **and N.I. Lebedev**[2]

[1] Astrophysikalisches Institut Potsdam, Telegrafenberg A 31, D-14473 Potsdam, Germany (Internet: KPflug@aip.de, KArlt@aip.de)
[2] Institute of Terrestrial Magnetism, Ionosphere and Radio Wave Propagation of the Russian Academy of Sciences, Troitsk City, Moscow Region, 142092 Russia (Internet: SolTer@charley.izmiran.rssi.ru)

Received 7 March 1996 / Accepted 17 June 1996

Abstract. Solar irradiance measurements with the DIFOS-photometer aboard the satellite CORONAS-I were compared with short term variations of solar activity. The sunspot blocking effect was confirmed and an anticorrelation with the 2600 MHz radio flux is very pronounced. Furthermore a close relation to the large scale structure of the magnetic field existed during the observational period from 1994, March 16 to May 7.

Key words: space vehicles – Sun: oscillations; activity; magnetic fields; general

1. Introduction

Solar irradiance measurements were carried out with the DIFOS experiment aboard the Russian-Ukrainian solar satellite CORONAS-I. The DIFOS photometer measured solar intensity integrated over the whole solar disk in three wavelength ranges. Detectors are silicon photodiodes. First of all DIFOS should measure global solar oscillations between 1 and 10 mHz. In 1991 Oraevsky and Zhugzhda published a description of the CORONAS-I satellite. In 1995 Lebedev et al. published an overview about the DIFOS-photometer and first results concerning solar irradiance oscillations.

In the present paper we use DIFOS observations for an estimate of short term solar irradiance variations between fractions of a day up to two solar rotations. In these time spans several authors investigated relations between solar irradiance variations and phenomena of activity. Mostly total irradiance measurements with ACRIM radiometers (Pap 1985, Pap et al. 1994) were used. It was found that generally sunspots cause a decrease and facula areas give an enhancement of solar luminosity. But details are complicated and an analysis of the DIFOS period between 1994, March 16 and May 7 is justified.

Send offprint requests to: K. Pflug

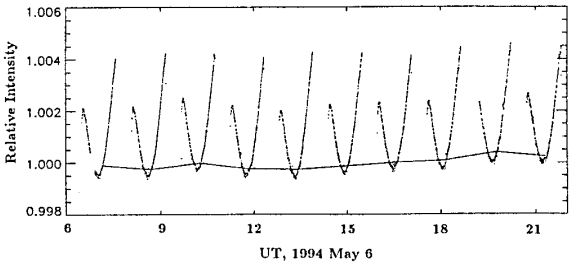

Fig. 1. Example of DIFOS raw data over 10 satellite orbits from the window 400–1000 nm. The curve connects mean values of each orbit.

2. Data analysis

Data sets from the DIFOS photometer contain full disc solar intensities in the wavelength ranges:
- around 550 nm with a bandpass of 100 nm,
- around 750 nm with a bandpass of 100 nm and
- from 400 nm to 1100 nm defined by the spectral sensitivity of the silicon photodiode.

They have a time resolution of 16 s. For 550 nm the data set starts only on March 25. The raw data are influenced by different disturbances, especially by variations of the photometer sensitivity in dependence on the temperature, degradation of the silicon photodiodes and different contributions from light scattered from the Earth's atmosphere into the measuring device.

The data reduction included the following two steps:

a) Calculation of the mean intensity during each orbit of the satellite. Therefore we used all measured values excluding 40% after leaving from and 30% before entering into the Earth's shadow (Fig. 1).

b) Elimination of the trend by use of polynomial approximations. In Fig. 2 one can find the resulting irradiance variation after a third order approximation for all channels.

Pflug et al. (1996) described this procedure in detail.

During the observational period we find a good correlation (coefficient 0.64) between the channels 400 - 1000 nm and 550 nm. The amplitudes are in both channels ≈ 0.003. The channel 750 nm is less correlated which will be discussed later.

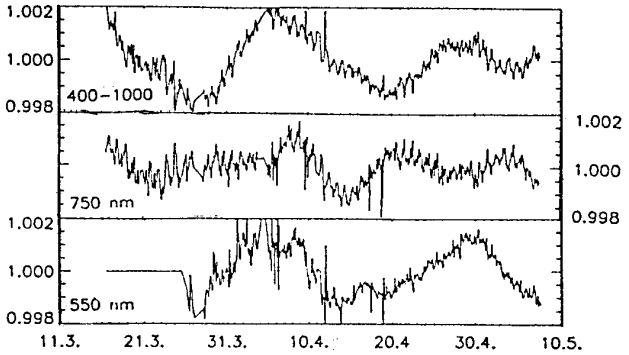

Fig. 2. DIFOS irradiance variation. Relative intensities are represented in the channels 400–1000 nm (above), 750 nm (centre), and 550 nm (below) in dependence on the time. The trend is eliminated by use of a 3-rd order polynomial.

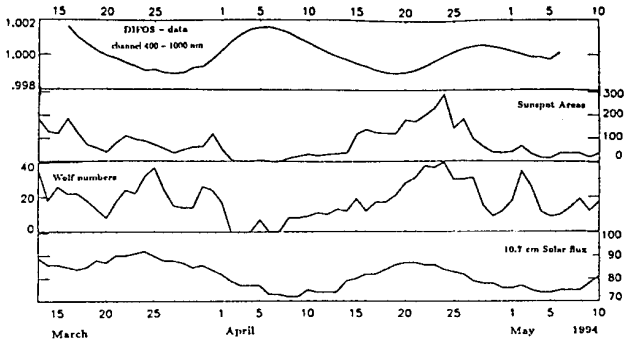

Fig. 3. Comparison between DIFOS irradiance variations and different parameters of solar activity. Represented are the DIFOS data for 400-1000 nm, the corrected sunspot areas in 10^{-6} of the hemisphere (mean values from different observatories), the international sunspot numbers, and the Penticton 2800 MHz (10.7 cm) solar flux in solar flux units. Data from Solar Geophysical Data.

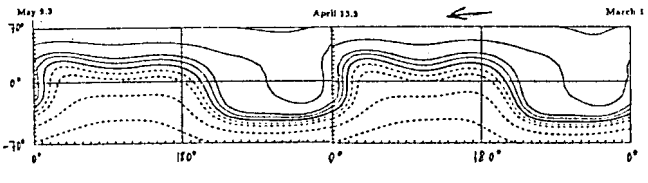

Fig. 4. Synoptic maps of the source surface magnetic field for the interval of the DIFOS records. Isolines correspond to 0, 1, 2, 5, 10, and 20 μTesla. Magnetic field data from the John Wilcox Observatory.

3. Relations to solar active phemomena

We find a pronounced recurrence of 27^d in all channels. This corresponds to a distinguished two sector structure of solar activity in 1994.

A comparison between sunspot numbers and sunspot areas confirms former results (see Fig. 3). In our time scales small activity corresponds to the maxima of solar irradiance. But this relation is not very pronounced. An anticorrelation with the 10.7 cm solar flux is much more distinguished (see also Fig. 3). Here a very good correspondence is to be found and a phase shift is suggested between both curves.

Finally we should mention the different behaviour of the infrared channel near 750 nm. In this spectral region we find a secondary minimum near April 27. One rotation before (near April 5) a small secondary minimum is also noticeable. This may be due to a stronger effect of chromospheric activity on this channel compared to the others. This spectral window is sensitive for three very strong CaII lines that are very sensitive to the solar plage activity. A more detailed analysis of this behaviour is planned.

4. Relation to the solar magnetic field

As demonstrated above, the DIFOS irradiance data are in anticorrelation with the solar activity parameters over the 27 days time scale. Now, it is useful to compare the DIFOS records with solar magnetic field data directly. However, before that, we should make some remarks.

It is widely known that a local and a global (or large–scale) magnetic field system exist on the Sun (Obridko 1983, Ivanov 1993, Grigoriev and Ermakova 1986). These fields, though closely connected, as a rule display different cyclic variation and different organization in space and in time. This difference is especially important when we deal with long term variations. In the case of the short range of DIFOS observations the difference between the two field systems should not strongly influence the analysis. Nevertheless, we would like to stress that we use magnetic field observations of very low resolution. Moreover, the mathematical method, applied to data processing, makes the resolution even lower and sometimes we shall use the fields of global scale.

4.1. Processing method

All components of the magnetic field at any point of a spherical layer, which extends from the photosphere to the so-called source surface, can be calculated in the potential approximation by using longitudinal magnetic field observations in the photosphere. We used the magnetic synoptic charts from the John Wilcox Observatory of Stanford University. The source surface is, by definition, a sphere where all field lines are radial. It is assumed to exist at a distance $R_s \simeq 2.5 R_\odot$ from the centre of the Sun.

The equations used to calculate the magnetic field components are written as follows:

$$B_r = \sum P_n^m(\cos\vartheta)(g_{nm}\cos m\varphi + h_{nm}\sin m\varphi) \\ ((n+1)(R_\odot/R)^{n+2} - n(R/R_s)^{n-1}c_n) \quad (1)$$

$$B_\vartheta = -\sum \frac{\partial P_n^m(\cos\vartheta)}{\partial\vartheta}(g_{nm}\cos m\varphi + h_{nm}\sin m\varphi) \\ ((R_\odot/R)^{n+2} + (R/R_s)^{n-1}c_n) \quad (2)$$

$$B_\varphi = -\sum \frac{m}{\sin\vartheta} P_n^m(\cos\vartheta)(h_{nm}\cos m\varphi - g_{nm}\sin m\varphi) \\ ((R_\odot/R)^{n+2} + (R/R_s)^{n-1}c_n) \quad (3)$$

Here, $0 \le m \le n < N$ (conventionally $N = 9$), $c_n = -(R_\odot/R_s)^{n+2}$, P_n^m are the Legendre polynomials,

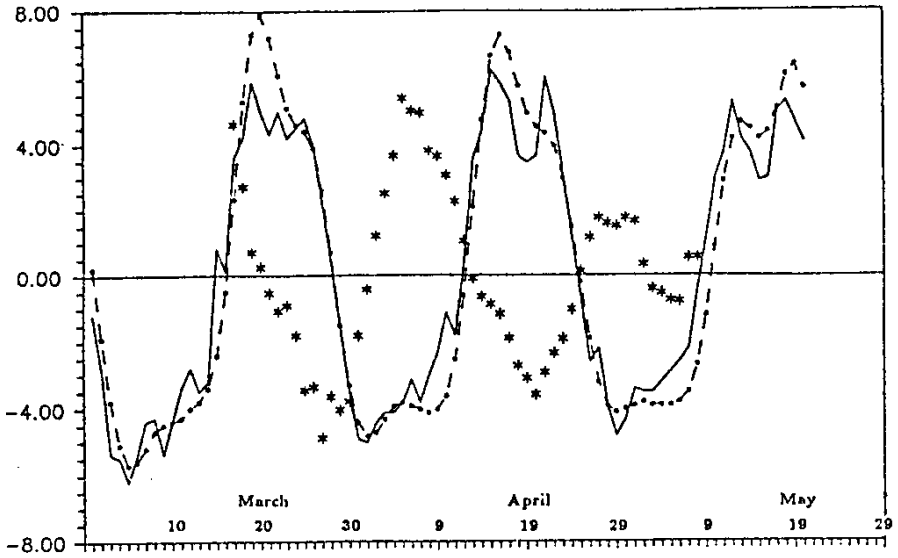

Fig. 5. Comparison with large–scale magnetic field indices. The source surface field, B_{ss}, is plotted in μTesla with a dash–dot line, and the mean solar magnetic field (Stanford) B_* is divided by 10 and plotted with a solid line. Data from the DIFOS channel 400-1000nm are plotted with asterisks.

g_{nm} and h_{nm} are the coefficients of the spherical harmonic analysis based on the original observational data. For the period under consideration, the coefficients were calculated directly from the synoptic maps.

According to Eqs. (1)–(3), the magnetic field can be calculated at every point between the photosphere and the source surface determined by three coordinates: the radial (R), azimuthal (φ), and meridional ones (θ).

4.2. Sector structure of the solar field

It is reasonable to begin the comparison with a global field of very large scale. Most convenient to our investigation is the field on the source surface. Here, the highest small–scale harmonics are automatically filtered out and only harmonics of the first and the second order are important.

Fig. 4 shows the synoptic maps of the source surface magnetic field during the two solar rotations when the DIFOS records were obtained. It is easy to see that the DIFOS records coincide in time with the very pronounced and extremely stable 2–sector structure of the global magnetic field. This, again, is in good agreement with the stable structure of the sunspot forming zone (see above). It accounts for the pronounced 27–day variation of all solar parameters and, as a result, of solar irradiance.

Now, let us compare the indices of large–scale magnetic fields. First, we compute the magnetic field B_{ss} at the intersection of the "Earth–Sun center" line with the source surface for every day. At the time of the DIFOS experiment this point was 7–5° southwards from the centre of the solar disk. Then, we compute the radial field component – the only present on the source surface. We compare the B_{ss} data with the everyday data on the Sun as the star B_* measured at Stanford and published in Solar–Geophysical Data. The results are represented in Fig. 5. We find that the two indices, B_{ss} and B_*, which are usually not alike, are very similar during the 53 days under consideration. The correlation coefficient is 0.956. It is again the effect of the very simple and stable structure of the large–scale magnetic field.

Coming back to the DIFOS data, we can see that the irradiance data are in anticorrelation with the magnetic data. The correlation coefficient is -0.467. At first sight, this result seems a bit strange. In fact, the solar irradiance variation should not be related to the sign of the solar magnetic field. This is only the result of our definition and depends on the observer's site. But the comparison, made in the following paragraph, makes the problem more clear.

4.3. Comparison of the photospheric and the source surface magnetic fields

Let us calculate the absolute value of the vector magnetic field at intersection of the "Earth–Sun's centre" line with the photosphere, B_{ph}. The difference between this and the point discussed above is that the B_{ss} field was calculated at the height of 2.5 solar radii and is strictly radial. As stated above, it is a very large–scale field, really global. The B_{ph} field is calculated at the same line, but in the photosphere. There are some shortcomings in these calculations that concern the influence of active regions (potential field approximation, low spatial resolution of 3' and use of the 9th order Legendre polynomials, which are not good enough to describe the real field structure in active regions). Consequently these calculations yield a mixed field intensity, which partially includes the large–scale and partially the local field. Therefore, we do not claim any actual physical meaning of our everyday calculation. However, we use as an index of field intensity in the photosphere the absolute value of the vector magnetic field.

Now, let us compare the B_{ph} and B_{ss} fields in Fig. 6. We see that during the period under investigation the days with large photospheric magnetic fields are in the positive, and those with weak fields in the negative sector. But the intervals with large

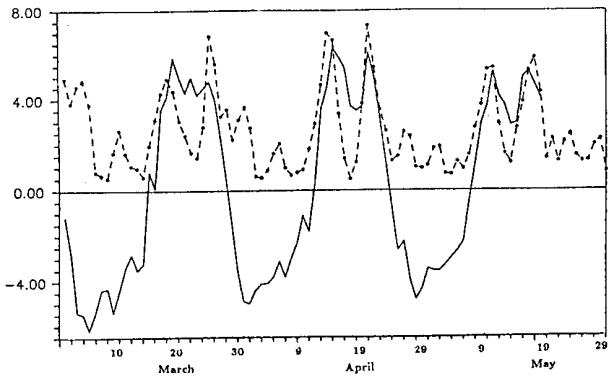

Fig. 6. Magnetic fields in the intersection of the "Earth-Sun centre" at the photosphere B_{ph} (dash-dotted line) and at a height of 2.5 solar radii B_{ss} (solid line). Ordinate in μTesla, for B_{ph} divided by 50.

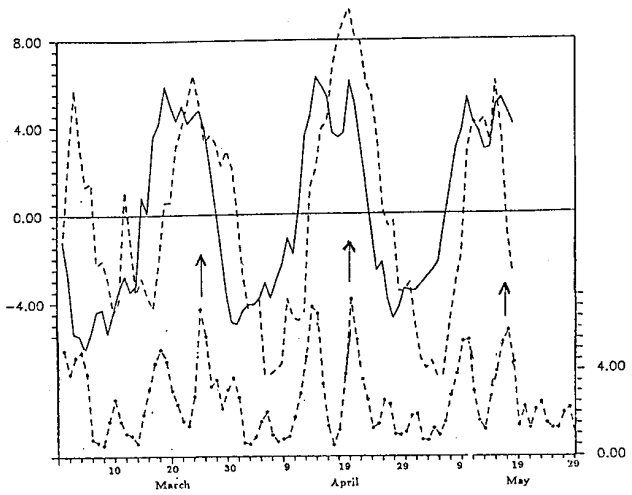

Fig. 7. Comparison between radio flux and magnetic field: *solid line* mean solar magnetic field B_* in μTesla, *dashed line* Penticton 2800 MHz solar flux after subtracting the 3rd–order trend. Flux variation between 70 and 90 sfu. *dash-dot line* below - Magnetic field at the photosphere B_{ph}, scale in μTesla at the right.

photospheric magnetic fields B_{ph} correspond to the minima of solar irradiance near March 28 and April 18.

4.4. Relationship between 2800 MHz solar flux, DIFOS "irradiance" data, and the magnetic field

Finally we compare the 2800 MHz solar flux variation with the magnetic field B_* (Sun as star). Both curves in the upper part of Fig. 7 are very similar to each other, but the radio flux curve is shifted by 3–4 days westwards from the magnetic curve. When matching the two curves we obtain an excellent correlation coefficient as large as 0.835.

The origin of the shift is not clear yet. Some hints at an explanation can be obtained by comparing the radio flux with the photospheric field, B_{ph} (dash–dot line in the lower part of Fig. 7). It is seen that the region of large magnetic fields has a fine two-maximum structure. The positive part of the radio flux (the days when it is larger than on the average) corresponds to the western maximum in the region of large fields (i.e. to the western part of the positive sector of the large–scale field - see Fig. 6). In Fig. 7 upwards arrows mark these points. On the contrary, the negative part of the radio flux (that means the deficit of the flux compared with the mean value) corresponds to the interval from weak fields up to the eastern maximum. Obridko et al. published a detailed version of the comparison between DIFOS irradiance data and magnetic fields in 1996.

5. Conclusions

We deduced our results from a short observational period of only two solar rotations. We analysed a period of low solar activity and stable two sector structure of the solar magnetic field. The correlation between the irradiance measurements, Wolf numbers and sunspot areas are in agreement with preceding investigations and the anticorrelation with the 2800 MHz solar flux is very pronounced.

The most remarkable finding is the anticorrelation between the global magnetic field and solar irradiance. The similarity between the curves of photospheric and global fields and DIFOS measurements may be a special result, only valid in times of low solar activity. We believe it to be the result of the global organization of fields in the Sun. This is especially pronounced during the declining phase of the cycle, when the global field controls the behaviour of all other solar activity indices.

Further steps are planned. We hope especially for a successful launching of the next CORONAS satellite carrying among others including an improved DIFOS photometer. Longer observational periods are very necessary for proving our results.

Acknowledgements. The authors gratefully acknowledge support of the present work by the German Space Agency (DARA) under grant No. 50 QL 9203 1.

References

Grigoriev, V.M. and Ermakova, L.V. 1986, Issled. po geomagnetismu, aeronomii i fizike Solntsa. M., Nauka, 25
Ivanov, E.V. 1993, In "Solar Terrestrial Energy Programme", COSPAR Colloquia Series 5, 133
Lebedev, N.I. et al. 1995, A&A 296, L25 - L28
Obridko, V.N. et al. 1996, Coronas Information No. 13
Oraevsky, V.N., Zhugzhda, Yu. 1991, Coronas Information No. 1
Pap, J.M. 1985, Solar Physics 97, 21
Pap, J.M. et al. 1994, Solar Physics 152, 13
Pflug, K. et al. 1996, Coronas Information No. 12

This article was processed by the author using Springer-Verlag LaTeX A&A style file *L-AA* version 3.